Genomic Basis for Resistance to BCL-2 Inhibition in Hematologic Malignancies

Genomic basis for resistance to BCL-2 inhibition in hematologic malignancies

by

Vivian Liu

Submitted in Partial Fulfillment of the Requirements for the M.D. Degree with Honors in a Special Field

February 4, 2019

Area of Concentration: Molecular Biology

Project Advisor: Catherine Wu, M.D.

Author's Prior Degrees: N/A

I have reviewed this thesis. It represents work done by the author under my supervision and guidance.

Abstract

B-cell chronic lymphocytic leukemia (CLL) is the most common adult leukemia in Western countries. The standard frontline therapy is a combination immune-chemotherapy, but relapse remains the rule for this disease. The treatment landscape of CLL and other B-cell malignancies is changing dramatically. Recently the FDA has approved the use of a BCL-2 inhibitor, venetoclax, to treat a subset of patients with relapsed CLL. Although this drug had a high response rate in clinical trials, clinical progression has been noted due to the development of drug resistance. Therefore, understanding the resistance mechanisms to this drug is a priority to glean maximum benefit from its use and to implement more personalized treatment strategies.

To study the mechanisms of venetoclax resistance in malignant B-cells, we used a genome-scale CRISPR-Cas9 screen of B-cell lines to determine the specific genes that are necessary for sensitivity to the drug. Our screen resulted in a total of 11 genes that are required for sensitivity to BCL-2 inhibition with venetoclax. Four of these genes are well-known pro-apoptotic genes in the apoptosis pathway (*PMAIP1*, *BAX*, *BAK1*, and *BCL2L11*). The other seven genes have relatively unknown function with respect to BCL-2 and apoptosis, and they have known functions of being transcription factors, transcriptional modulators, and ubiquitin modifiers. Isogenic cell lines with these genes knocked-out have confirmed resistance to venetoclax with increased IC50 values and increased rate of proliferation under drug treatment.

Transcriptomic and proteomic analysis of a lymphoma cell line with induced resistance to venetoclax demonstrated upregulation of MCL-1 and downregulation of ID2. Comparison transcriptomes of a resistant line and isogenic cell lines revealed the *ID3* knockout as the most similar to the resistant cell line. Further analysis revealed a resistance circuit involving ID3 repression and increased AMPK and PKA signaling as mechanisms of resistance in cell lines. Targeting AMPK and the mitochondrial electron transport chain (mETC) resulted in sensitization of cells to venetoclax. Whole exome sequencing of our resistant cell line along with pre- and post-venetoclax samples from 6 patients revealed a common amplification of chromosome 1q23 in both the resistant cell line and 3 of the 6 patients. This region contained the genes *MCL1* and *PRKAB2*. Immunohistochemistry studies revealed increased expression of MCL1 and AMPK signaling components in patient samples. These results provide greater insight into mechanisms of resistance to venetoclax and suggest MCL-1 inhibitors, AMPK inhibitors, and mETC modulators as possibilities for combination therapies to combat resistance.

Abbreviations

ABT-199: venetoclax
ACC: acetyl-CoA carboxylase
AML: acute myeloid leukemia
AMPK: adenosine monophosphate-activated protein kinase
BAK1: Bcl-2 homologous antagonist killer
BAX: Bcl-2-associated X protein
BCL-2: B-cell lymphoma 2
BCL-XL: B-cell lymphoma-extra large
BCL2L11(BIM): Bcl-2-like protein 11
BCR: B-cell receptor
BH3: Bcl-2 homology domain 3
BID: BH3 interacting domain death agonist
CCF: cancer cell fraction
CLL: chronic lymphocytic leukemia
CRISPR-Cas9: clustered regularly interspaced short palindromic repeats-CRISPR-associated 9
DMSO: dimethyl sulfoxide
EP300: histone acetyltransferase p300
FDA: Food and Drug Administration
ID2: inhibitor of DNA binding 2
ID3: inhibitor of DNA binding 3
IKZF5: IKAROS family zinc finger 5
LFC: log fold change
LOF: loss of function
MCL-1: myeloid cell leukemia sequence 1
mTOR: mammalian target of rapamycin
mETC: mitochondrial electron transport chain
NFIA: nuclear factor 1 A
NFKBIA: NFKB inhibitor alpha
OCI-Ly1-S: OCI-Ly1-Sensitive
OCI-Ly1-R: OCI-Ly1-Resistant
OTUD5: ovarian tumor deubiquitinase 5
PI3K: phosphoinositide 3-kinase
PKA: protein kinase A
PMAIP1: Phorbol-12-Myristate-13-Acetate-Induced Protein 1
sgRNA: single guide ribonucleic acid
shRNA: short hairpin ribonucleic acid
sCNVs: somatic copy number variations
sSNVs: somatic single-nucleotide variations
TP53: tumor protein 53
UBR5: ubiquitin protein ligase E3 Component N-Recognin 5
WES: whole-exome sequencing

other BCL-2 family members such as BCL-XL[11]. Currently, the most successful BCL-2 inhibitor is venetoclax (ABT-199), a BH3 mimetic that binds BCL-2 with more specificity than previous BCL-2 inhibitors[12] and triggers apoptosis in a TP53-independent manner[13]. In humans, a phase 1 trial of venetoclax in CLL patients with relapsed disease noted an overall response rate of 79% and 20% with complete remission[14]. Notably, patients with unfavorable genetic alterations of *TP53*, such as a 17p deletion or *TP53* gene mutation, responded at a similar rate as those patients without any *TP53* perturbation, consistent with previous studies showing that venetoclax acts independently of TP53[14]. Due to these results, in April 2016 the FDA granted accelerated approval to venetoclax for use in CLL patients with a 17p deletion and had previously undergone at least one therapy[15]. Most recently in November 2018, the FDA granted accelerated approval to venetoclax in combination with azacitidine or decitabine or low-dose cytarabine for newly-diagnosed acute myeloid leukemia (AML) in adults aged 75 years or older, or who have comorbidities that preclude use of intensive induction chemotherapy. Further clinical trials are currently being conducted to expand the use of this drug. Although these results are exciting, clinically evident resistance has been noted, with the rate of progression at 15 months of 33% in the CLL trial participants[14]. Therefore, as more and more patients are being treated with venetoclax, it is important to understand the mechanisms of resistance so that this drug can be used to its full potential.

Current Understanding of Resistance to BCL-2 Inhibition

The factors contributing to resistance to venetoclax in patients remain unclear. One possible mechanism of resistance is the upregulation of other anti-apoptotic BCL-2 family members, which has been shown in various *in vitro* models. In lymphoma cell lines, increased expression of other BCL-2 family members (e.g. MCL-1, BCL-XL, and BFL-1) has been linked to resistance to venetoclax and other BH3 mimetics[16]. In CLL cells, the upregulation of BCL-XL and BCL2A1 has been shown to induce resistance to the BH3 mimetic ABT-737[17]. Subsequent studies have suggested various strategies for overcoming this type of resistance. In CLL and lymphoma models, inhibiting BCR signaling and preventing PI3K/AKT/mTOR activation were shown to counter MCL-1 mediated resistance to varying degrees[18,19]. In an AML model, targeting MCL-1 and BCL-XL has been shown to counteract the acquisition of venetoclax resistance[20]. In addition, a screen of kinase inhibitors identified sunitinib (a multi-targeted

Study Aims

In this study, we apply this new technological advance to determine the genes involved in venetoclax resistance. The genome-scale CRISPR-Cas9 screen allows for the identification of genes which lead resistance to venetoclax when their expression is deregulated. In addition, transcriptomic and proteomic analysis of a venetoclax-resistant will help to inform of the gene expression changes that occur from *in vitro* acquired resistance to the drug. Finally, whole-exome sequencing of paired patient samples before and after venetoclax resistance will help to guide the clinical relevance of our findings. Overall, this study aims to increase the understanding of venetoclax resistance in B-cell malignancies as well as expand the understanding of components of the apoptosis pathway.

DHL4 resistance line. SU-DHL4 (ATCC), SU-DHL6 (Letai lab), Toledo (ATCC) cells were cultured in Roswell Park Memorial Institute media (Gibco) supplemented with 10% FBS and 1% penicillin/streptomycin.

Drugs: Venetoclax (ABT-199; Selleck Chemicals), dorsomorphin (Sigma), oligomycin A (Sigma), antimycin A (Sigma), and AMPK activator A-769662 (Santa Cruz Biotechnology) were used for drug treatment experiments. All drugs were resuspended in DMSO (Sigma).

Cell viability assays: The Cell Titer-Glo Luminescent Cell Viability Assay (Promega) was used to determine the relative number of viable cells after drug treatment. 0.2 × 106 cells/mL were seeded in a 24 well-plate and treated with drugs for 24 or 48 hours. The viability assay was conducted using the manufacturer's protocol after treatment. Values were normalized to DMSO-treated cells. Plates were read on a SpectraMax M3 reader (Molecular Devices).

Western blotting

Total protein from cells was isolated using RIPA Buffer (20 mM Tris-HCl pH 7.5, 150 mM NaCl, 1mM Na_2EDTA, 1 mM EGTA, 1% NP-40, 1% sodium deoxycholate, 2.5 mM sodium pyrophosphate, 1 mM ß-glycerophosphate, 1mM Na_3VO_4, 1ug/mL leupeptin), supplemented with protease inhibitors (Thermo Fisher Scientific) and phosphatase inhibitors (Thermo Fisher Scientific). Protein concentration was determined with the BCA Protein Assay (Pierce). Protein samples (25 μg) were separated on either 4-12% Bis-Tris gels (proteins <250 kDa) or Tris-acetate gels (proteins >250 kDa). Protein was transferred to a nitrocellulose or PVDF membrane (Life Technologies) using the iBlot2 system (Life Technologies). Membranes were incubated overnight with primary antibodies recognizing BCL-2 (1:1000; Abcam), MCL-1 (1:200; Santa Cruz), BCL-XL (1:100; Santa Cruz), BIM (1:1000; Cell Signaling Technology), BAK (1:1000; Cell Signaling Technology), BAX (1:1000; Cell Signaling Technology), Pegasus (1:1000; Santa Cruz), OTUD5 (1:1000; Cell Signaling Technology), NOXA (1:100; Santa Cruz), ID3 (1:1000; Cell Signaling Technology), ID2 (1:1000; Cell Signaling Technology), p300 (1:1000; Santa Cruz), UBR5 (1:1000; Cell Signaling Technology), IκBα (1:1000; Cell Signaling Technology), NF-1 (1:200; Santa Cruz), and GAPDH (1:1000; Cell Signaling Technology). After incubation in the appropriate secondary antibodies (anti-rabbit IgG, 1:5000, HRP-linked,

filtered through a 0.45 μm low protein binding membrane (Millipore Steriflip HV/PVDF) and added to 1 mL of LentiX Concentrator (Clontech). This mixture was then incubated at 4°C for 2 h, and centrifuged at 1500×g for 45 min at 4°C. The pellet was resuspended in 100 μL of PBS and stored in aliquots at –80°C.

Generation of engineered cell lines

0.5×10^6 target OCI-Ly1 cells were suspended in media supplemented with 8 μg/mL polybrene and seeded into 6-well plates (1 mL per well), to which lentivirus was added (50 μL/mL to each well). The plates were spun at 2000 rpm for 2 h at 37ºC and incubated at 37ºC for 24 h. The polybrene-containing media was then replaced by 2 mL of fresh media per well. After 3 days, transduced cells were selected (i.e. by puromycin (1 μg/mL) for 1 week for the ORF-overexpressing cells) or sorted (i.e. based GFP or mCherry expression for the CRISPR gene-edited lines) and cryopreserved for further experiments. As confirmation that the engineered cell lines expressed the expected alterations, expression of the targeted protein by western blot before and after 2 weeks of exposure to venetoclax 100 nM.

RNA sequencing

cDNA Library Construction

Total RNA was quantified using the Quant-iT RiboGreen RNA Assay Kit and normalized to 5 ng/μl. Following plating, 2 μL of ERCC controls (using a 1:1000 dilution) were spiked into each sample. An aliquot of 200ng for each sample was transferred into library preparation which uses an automated variant of the Illumina TruSeq Stranded mRNA Sample Preparation Kit. This method preserves strand orientation of the RNA transcript. It uses oligo dT beads to select mRNA from the total RNA sample, followed by heat fragmentation and cDNA synthesis from the RNA template. The resultant 400bp cDNA then goes through dual-indexed library preparation: 'A' base addition, adapter ligation using P7 adapters, and PCR enrichment using P5 adapters. After enrichment, the libraries were quantified using Quant-iT PicoGreen (1:200 dilution). After normalizing samples to 5 ng/μL, the set was pooled and quantified using the KAPA Library Quantification Kit for Illumina Sequencing Platforms. The entire process was in a 96-well format and all pipetting is done by either Agilent Bravo or Hamilton Starlet.

Tandem Mass Tag labeling of peptides

Desalted peptides were labeled with tandem mass tag (TMT) 10-plex isobaric mass tagging reagents (Thermo Fisher Scientific) as previously described [29]. Each TMT reagent was resuspended in 41 µL of MeCN. Peptides were resuspended in 100 µL of 50 mM HEPES and combined with TMT reagent. Samples were incubated at RT for 1 h while shaking. The TMT reaction was quenched with 8 µL of 5% hydroxylamine at RT for 15 min with shaking. TMT labeled samples were combined, dried to completion, reconstituted in 100 µL of 0.1% FA, and desalted on StageTips or 100 mg SepPak columns as described above.

Basic Reverse Phase (bRP) Fractionation

The TMT labeled samples were fractionated using offline high pH reversed-phase chromatography (bRP) as previously described [29]. Samples were fractionated using Zorbax 300 Extend C18 column (4.6 × 250 mm, 300 Å, 5 µm, Agilent) on an Agilent 1100 series high-pressure liquid chromatography (HPLC) system. Samples were reconstituted in 900 µL of 5 mM ammonium formate (pH 10.0)/2% (vol/vol) acetonitrile (MeCN) (bRP solvent A). Samples were injected with Solvent A at a flow rate of 1 mL/min and separated using a 96 min gradient. The gradient consisted of an initial increase to 16% solvent B (90% MeCN, 5 mM ammonium formate, pH 10), followed by 60 min linear gradient from 16% solvent B to 40% B and successive ramps to 44% and 60% at a flow rate of 1 mL/min. Fractions were collected in a 96-deep well plate (GE Healthcare) and pooled in a non-contiguous manner into final 24 proteome fractions. Pooled fractions were dried to completeness using a SpeedVac concentrator.

Liquid chromatography and mass spectrometry

Desalted peptides were resuspended in 9 µL of 3% MeCN/0.1% FA and analyzed by online nanoflow liquid chromatography tandem mass spectrometry (LC-MS/MS) using Q-Exactive + mass spectrometer (Thermo Fisher Scientific) coupled on-line to a Proxeon Easy-nLC 1200 (Thermo Fisher Scientific) as previously described[29]. Briefly, 4 µL of each sample was loaded onto a microcapillary column (360 µm outer diameter × 75 µm inner diameter) containing an integrated electrospray emitter tip (10 µm), packed to approximately 22 cm with ReproSil-Pur C18-AQ 1.9 µm beads (Dr. Maisch GmbH) and heated to 50 ºC. Samples were analyzed with

implemented in R-Shiny using the limma R library. Correction for multiple testing was performed using the Benjamini-Hochberg false discovery rate method.

Human samples

(prepared by Stacey M. Fernandes)

Genomic DNA was isolated (DNAeasy Blood and Tissue Kit, Qiagen) from specimens collected from CLL patients enrolled on clinical trials of venetoclax treatment (NCT01328626, NCT02141282), approved by and conducted in accordance with the principles of the Declaration of Helsinki and with the approval of the Institutional Review Boards (IRB) of the University of Texas/MD Anderson Cancer Center (MDACC; Patients 1, 3, 4) or of Dana-Farber Cancer Institute (DFCI; Patient 2, 5, 6). Their clinical characteristics are reported in **Table 3**. Blood and/or tissue tumor samples were collected at baseline, before initiation of venetoclax therapy, and at relapse or progression on venetoclax (**Table 4**).

Whole-exome sequencing and data analyses

(performed by Romain Guièze, Daniel Rosebrock, Aina Martinez, and Dimitri Livitz under the supervision of Ignaty Leshchiner and Gad Getz)

Library construction from CLL and matched germline DNA of Patients 1–6 was performed as previously described[30], with the following modifications: (i) initial genomic DNA input into shearing was reduced from 3 μg to 10–100 ng in 50 μl of solution; (ii) for adapter ligation, Illumina paired-end adapters were replaced with palindromic forked adapters (from Integrated DNA Technologies), with unique dual-indexed molecular barcode sequences included in the adapter sequence to facilitate downstream pooling. With the exception of the palindromic forked adapters, the reagents used for end repair, A-base addition, adapter ligation and library enrichment PCR were purchased from KAPA Biosciences in 96-reaction kits, (iii) during the post-enrichment solid-phase reversible immobilization (SPRI) cleanup, elution volumes were reduced to 30 μL to maximize library concentration, and a vortexing step was added to maximize the amount of template eluted. Any libraries with concentrations below 40 ng/ml (per PicoGreen assay, automated on an Agilent Bravo) were considered failures and reworked from the start of the protocol. Following library construction, hybridization and capture were performed using the relevant components of Illumina's Nextera Rapid Capture Exome Kit and following the

measurement was used in MuTect. From the aligned BAM files, somatic alterations were identified using a set of tools developed at the Broad Institute (www.broadinstitute.org/cancer/cga). The details of our sequencing data processing have been described elsewhere[34,35].

Following our standard procedure, sSNVs were detected using MuTect[9] (version 1.1.6); sINDELs were detected using Strelka[36]. We then applied a stringent set of filters to improve the specificity of our sSNV and sINDEL calls and remove likely FFPE artifacts. We applied an allele fraction specific panel-of-normals filter, which compares the detected variants to a large panel of normal exomes and removes variants that were observed in the panel-of-normals. We then applied a realignment based filter, which removes variants that can be attributed entirely to ambiguously mapped reads. All filtered events in candidate CLL genes were also manually reviewed using the Integrated Genomics Viewer (IGV)[37]. In the matched sample sets from 6 individuals, we utilized "forced calling" to quantify the number of reads supporting the alternate and reference alleles at sites which were detected in any sample from that individual. Estimation of and correction for tumour contamination in normal was performed using the deTiN algorithm [38] to recover somatic mutations that would have otherwise been filtered out due to evidence of the mutation in the normal. To address the lack of a matched normal sample (in Patient 3) we used a stringent panel-of-normals and population allele frequency criteria, and excluded non-coding variants from analysis. To address the lack of a matched normal sample (in Patient 6), we used a stringent panel-of-normals and population allele frequency criteria, and excluded non-coding variants from analysis. Furthermore, parental OCI-Ly1-S cells were used as a source control DNA in order to highlight sSNVs that were acquired in the resistant OCI-Ly1-R cells. Reference lists for sSNVs and sINDELs in known putative CLL driver genes as well as for recurrent CNAs were concatenated based on previous sequencing studies of large CLL cohorts[39–43]. Total copy number was measured using ReCapSeg (www.broadinstitute.org/cancer/cga), then segmented into allelic copy number with AllelicCapSeg[44] based on heterozygous germline sites detected with HaplotypeCaller according to the protocol described previously (http://archive.broadinstitute.org/cancer/cga/acsbeta).

trained by a pathologist to identify tumor cells that were positive for each of the targets above. A percentage of the total tumor cells identified that are positive for the stain of interest is given.

UBR5 in 18% of mantle cell lymphomas[50], *ID3* in 68% of Burkitt lymphomas[51], and *NFKBIA* in 20% of Hodgkin lymphomas[52]. None of these 7 candidate genes have a known role in the regulation of apoptosis or have been previously implicated in venetoclax resistance.

Validation of screen results through the generation of isogenic knockout cell lines

To confirm the LOF screen results, single-gene knockout OCI-Ly1 cell lines for each of the 11 gene hits were generated. For each gene, 2 cell lines were generated from the 2 most efficient sgRNAs. Four control lines were also generated using 2 non-targeting sgRNAs and for 2 sgRNAs targeting *TP53*. Across the individual knockout cell lines, there was a decreased sensitivity to venetoclax with median increase in IC50 of 2.1-fold (range, 1.3- to 13.8-fold; $P < 0.05$, extra-sum-of-squares F test) compared to cell lines transduced with non-targeting control sgRNAs (**Figure 4A-B**). Moreover, all generated knockout and overexpression lines showed increased cumulative growth over 10 days of *in vitro* venetoclax treatment compared to control lines (**Figure 4C**). Exposure of the knockout cell lines to venetoclax increased the degree of depletion of the targeted protein (**Figure 4D**). In addition, levels of expression of MCL-1 were not increased in the knockout cell lines either before or after selection with venetoclax (**Figure 4E**). Altogether, these results confirmed the on-target effects of the sgRNAs identified in the LOF screen and suggest that repression of these genes result in an MCL-1 independent mechanism of resistance.

Venetoclax resistance signature involves MCL-1 overexpression, ID2 repression, and changes cellular energy metabolism

To study the resistance signature of *de novo* venetoclax resistance acquired *in vitro,* a venetoclax-resistant cell line was generated via chronic *in vitro* drug exposure of the parental cell line until the cells were able to grow in 1 μM venetoclax. This chronic drug exposure generated a resistant cell line (OCI-Ly1-R) with a significantly higher IC50 (1 μM) than the parental cells (4 nM) (**Figure 5A**). To determine the changes in gene and protein expression in the resistant cell line, the transcript and protein expression profiles of the OCI-Ly1-R cell line were characterized. Through RNA-sequencing of the resistant and sensitive cell lines, we identified 19 upregulated and 28 downregulated genes (adjusted P-value < 0.05; |LFC| > 2) (**Figure 5B**). Proteomic analysis of the resistant and sensitive cell lines was also performed with mass spectrometry-

Through comparison of the transcriptomic profiles of the *ID3* knockout cell line and the nontargeting control line, the PKA (protein kinase A) subunit *PRKAR2B* was the most significantly upregulated gene of the *ID3* knockout cell line (adjusted *P*-value < 0.05, LFC > 2; **Figure 6B**). Other strongly dysregulated transcripts fell in the mTOR pathway (e.g. *DEPTOR* [DEP domain-containing mTOR-interacting protein] gene), the Ras signaling pathway (*DIRAS1*, *RHOB, GNG7, SYNGAP1* genes), and B-cell differentiation (*EGR1*, *EGR2*). Because of the upregulation of PKA in the ID3 knockout line and additional data from the lab implicating involvement of AMPK overexpression in venetoclax resistance, two OCI-Ly1 cell lines were generated to overexpress *PRKAR2B* (a PKA subunit) and *PRKAA2* (the catalytic AMPK subunit) by Kaitlyn Baranowski, a research technician in the lab. Overexpression of either PKA or AMPK led to repression of both ID3 and ID2 (**Figure 6C**). In addition, the PKA and AMPK overexpressing cells both demonstrated increased sensitivity to the combination of venetoclax and oligomycin, an inhibitor of mETC (**Figure 6D**). The AMPK overexpressing line also showed increased sensitivity to the combination of venetoclax and dorsomorphin, an AMPK inhibitor (**Figure 6D**). Single cell clones derived from the ID3 knockout cell line were more sensitive to the combination of venetoclax and either dorsomorphin or oligomycin than control cells (**Figure 6E**).

Targeting AMPK signaling and the mETC also had effects on the OCI-Ly1-S and OCI-Ly1-R cell lines. Treatment of OCI-Ly1-R with either dorsomorphin or oligomycin (conducted by María Hernández-Sánchez) was able to sensitize the resistant cells to venetoclax (**Figure 7A**). Similar sensitization to venetoclax was seen with a second cell line SU-DHL4, was rendered resistant to venetoclax in a similar manner (**Figure 7B**). In a similar vein, when OCI-Ly1-S cells were treated with combination drugs, dorsomorphin and oligomycin synergized with venetoclax (**Figure 7C**), and similar results were seen in other venetoclax-sensitive lymphoid cell lines SU-DHL4, SU-DHL6, and Toledo (**Figure 7D**). Finally, the addition of small molecule AMPK-activator A-769662 to OCI-Ly1-S cells and 2 other venetoclax-sensitive lymphoid cell lines (SU-DHL6 and Toledo) resulted in a decrease in sensitivity to venetoclax (**Figure 7E**). These observations connect the results of the LOF screen and identify a venetoclax resistance circuit involving AMPK/PKA overexpression and ID3 repression.

Discussion

Mechanisms of venetoclax resistance in patients have been difficult to study thus far due to the scarcity of patient samples before and after relapse. Generally, relapse occurs in bone marrow or lymph nodes, making obtaining relapse samples more challenging as the disease is not circulating in the periphery. Therefore, for this study, we used an unbiased genome-scale loss-of-function screen, characterization of a resistant cell line model, and analysis of 6 paired CLL patient samples to uncover candidate drivers of venetoclax resistance.

The loss-of-function genome-scale screen uncovered a total of 11 candidate genes that result in resistance when underexpressed, four of which encode expected pro-apoptotic proteins and the other 7 of which encode genes not previously implicated in this pathway. In conjunction, the transcriptomic and proteomic analysis of the resistant cell line confirmed alterations leading to overexpression of MCL-1 at both the RNA and protein level, resulting in the ability to sequester BIM and compensate for BCL-2 inhibition, which is a previously-reported in vitro mechanism of resistance to this drug[20,54,58]. However, while upregulation of MCL-1 was demonstrated in the *in vitro* resistant cell line, it was not seen in any of the single knock-out lines of the genes uncovered in the LOF screen, indicating an alternative mechanism of resistance in these cells.

Comparison of the transcriptomic changes resistant cell line and those from the non-BCL-2 family member knock-out cell lines revealed a resistance circuit involving ID3 repression and AMPK/PKA overexpression. In addition, modulators of AMPK activity and mETC affected the sensitivity of cells to venetoclax, indicating a change in regulation of metabolism via the mETC. We show that this metabolic regulation depends on repression of the ID family of lymphoid transcriptional regulators. These results mesh well with recent work demonstrating that lymphoid transcription factors function as metabolic gatekeepers by limiting the amount of cellular ATP to levels that are insufficient for malignant transformation[55]. Hence, although our studies focused on the impact of ID3, a broader involvement of altered lymphoid differentiation state on venetoclax resistance is anticipated since repression of additional lymphoid transcription factors (IKZF5, EP300) were identified in our knockout screen. We also report a common amplification of chromosome 1q23 in both our resistance cell lines and 3 of 6 patients, which encompasses a region containing both *MCL1* and AMPK regulatory subunit *PRKAB2*, providing a genetic basis for resistance in patients. In addition, the pattern of immunohistochemical

therapies. These data support the possibility of targeting MCL-1 with emerging inhibitors as well as using AMPK inhibitors or mETC modulators to combat resistance.

While this study uncovered 7 non-BCL-2 family member genes that result in resistance to venetoclax, we mainly focused on the *ID3* knockout due to its similarity in transcriptome to our resistant cell line. Further transcriptomic and proteomic analysis of the other isogenic knockout lines that were generated could help to either reveal other pathways to venetoclax resistance or unveil further regulators of AMPK and PKA signaling. In addition, protein expression of AMPK and PKA can be shown via western blot to determine whether the other isogenic cell lines also result in changes in AMPK and PKA.

Another area that could be further strengthened is the connection between our cell line data and patient data. For instance, either RNA sequencing or targeted quantitative RT-PCR of RNA collected from patients before and after development of resistance to venetoclax could be performed to look at the expression of our candidate genes and AMPK/PKA signaling components, which could help to reinforce our results from our cell lines. Another possibility is to treat primary CLL cells from patients with the AMPK signaling and mETC modulators used on the cell lines to show that venetoclax sensitivity is also altered in primary CLL samples when either AMPK signaling or the mETC is disturbed.

Summary

CLL is a disease in which newly developed targeted therapies are drastically changing the treatment landscape of the disease. In particular, the BCL-2 inhibitor venetoclax has both shown promising efficacy as well as clinically-evidence resistance. However, studying venetoclax resistance has been challenging due to the paucity of patient samples after relapse. In this study, we used a genome-wide loss-of-function screen to uncover candidate genes that result in resistance when underexpressed. We also used genomic, transcriptomic, and proteomic analysis to determine the resistance mechanism of a resistant cell line. Finally, we analyzed tissue samples from patients before and after development of venetoclax resistance. These three approaches combined unveiled a resistance circuit involving AMPK and PKA overexpression and ID3 repression and changes in venetoclax sensitivity when used in combination with AMPK and mETC modulators. These results raise the possibility of venetoclax affecting the

Acknowledgements

I would like to thank my thesis advisor, Dr. Catherine Wu, who has consistently provided me support and guidance in my research and beyond. I would also like to thank my post-doctoral mentor, Dr. Romain Guièze, with whom I worked closely for this project and provided me scientific input.

This project involved extensive collaboration with various individuals with specific areas of expertise. I would like to thank all of those involved in this project for their work and helpful feedback: Daniel Rosebrock, María Hernández-Sánchez, Aina Martinez, Jing Sun, Kaitlyn Baranowski, Zachary Cartun, Ozan Aygün, Dimitri Livitz, J. Bryan Iorgelescu, Wandi Zhang, Stacey M. Fernandes, Ana Lako, Zoe B. Ciantra, Namrata D. Udeshi, Anthony G. Letai, Donna Neuberg, J. Wade Harper, Steven A. Carr, Federica Piccioni, Ignaty Leshchiner, Cory M. Johannessen, John Doench, Gad Getz. I would also like to thank the entire Wu lab for welcoming me and helping me on a day-to-day basis.

I am also grateful to the American Society of Hematology HONORS (Hematology Opportunities for the Next Generation of Research Scientists) Award, Harvard-MIT Health Sciences and Technology program, and the Harvard Medical School Scholars in Medicine Office for providing funding for this thesis.

12. Souers, A. J. *et al.* ABT-199, a potent and selective BCL-2 inhibitor, achieves antitumor activity while sparing platelets. *Nat. Med.* **19**, 202–208 (2013).
13. Anderson, M. A. *et al.* The BCL2 selective inhibitor venetoclax induces rapid onset apoptosis of CLL cells in patients via a TP53-independent mechanism. *Blood* **127**, 3215–3224 (2016).
14. Roberts, A. W. *et al.* Targeting BCL2 with Venetoclax in Relapsed Chronic Lymphocytic Leukemia. *N. Engl. J. Med.* **374**, 311–322 (2016).
15. Del Poeta, G. *et al.* Venetoclax: Bcl-2 inhibition for the treatment of chronic lymphocytic leukemia. *Drugs Today Barc. Spain 1998* **52**, 249–260 (2016).
16. Yecies, D., Carlson, N. E., Deng, J. & Letai, A. Acquired resistance to ABT-737 in lymphoma cells that up-regulate MCL-1 and BFL-1. *Blood* **115**, 3304–3313 (2010).
17. Vogler, M. *et al.* Concurrent up-regulation of BCL-XL and BCL2A1 induces approximately 1000-fold resistance to ABT-737 in chronic lymphocytic leukemia. *Blood* **113**, 4403–4413 (2009).
18. Bojarczuk, K. *et al.* BCR signaling inhibitors differ in their ability to overcome Mcl-1-mediated resistance of CLL B cells to ABT-199. *Blood* **127**, 3192–3201 (2016).
19. Choudhary, G. S. *et al.* MCL-1 and BCL-xL-dependent resistance to the BCL-2 inhibitor ABT-199 can be overcome by preventing PI3K/AKT/mTOR activation in lymphoid malignancies. *Cell Death Dis.* **6**, e1593 (2015).
20. Lin, K. H. *et al.* Targeting MCL-1/BCL-XL Forestalls the Acquisition of Resistance to ABT-199 in Acute Myeloid Leukemia. *Sci. Rep.* **6**, 27696 (2016).
21. Oppermann, S. *et al.* High-content screening identifies kinase inhibitors that overcome venetoclax resistance in activated CLL cells. *Blood* **128**, 934–947 (2016).
22. Fresquet, V., Rieger, M., Carolis, C., García-Barchino, M. J. & Martinez-Climent, J. A. Acquired mutations in BCL2 family proteins conferring resistance to the BH3 mimetic ABT-199 in lymphoma. *Blood* **123**, 4111–4119 (2014).
23. Blombery, P. *et al.* Acquisition of the recurrent Gly101Val mutation in BCL2 confers resistance to venetoclax in patients with progressive chronic lymphocytic leukemia. *Cancer Discov.* CD-18-1119 (2018). doi:10.1158/2159-8290.CD-18-1119
24. Shalem, O. *et al.* Genome-scale CRISPR-Cas9 knockout screening in human cells. *Science* **343**, 84–87 (2014).

40. Quesada, V. *et al.* Exome sequencing identifies recurrent mutations of the splicing factor SF3B1 gene in chronic lymphocytic leukemia. *Nat. Genet.* **44**, 47–52 (2012).
41. Landau, D. A. *et al.* Evolution and Impact of Subclonal Mutations in Chronic Lymphocytic Leukemia. *Cell* **152**, 714–726 (2013).
42. Puente, X. S. *et al.* Non-coding recurrent mutations in chronic lymphocytic leukaemia. *Nature* **526**, 519–524 (2015).
43. Landau, D. A. *et al.* Mutations driving CLL and their evolution in progression and relapse. *Nature* **526**, 525–530 (2015).
44. Stachler, M. D. *et al.* Paired exome analysis of Barrett's esophagus and adenocarcinoma. *Nat. Genet.* **47**, 1047–1055 (2015).
45. Carter, S. L. *et al.* Absolute quantification of somatic DNA alterations in human cancer. *Nat. Biotechnol.* **30**, 413–421 (2012).
46. Roemer, M. G. M. *et al.* Classical Hodgkin Lymphoma with Reduced β2M/MHC Class I Expression Is Associated with Inferior Outcome Independent of 9p24.1 Status. *Cancer Immunol. Res.* **4**, 910–916 (2016).
47. Carey, C. D. *et al.* Topological analysis reveals a PD-L1-associated microenvironmental niche for Reed-Sternberg cells in Hodgkin lymphoma. *Blood* **130**, 2420–2430 (2017).
48. Morin, R. D. *et al.* Frequent mutation of histone-modifying genes in non-Hodgkin lymphoma. *Nature* **476**, 298–303 (2011).
49. Pastore, A. *et al.* Integration of gene mutations in risk prognostication for patients receiving first-line immunochemotherapy for follicular lymphoma: a retrospective analysis of a prospective clinical trial and validation in a population-based registry. *Lancet Oncol.* **16**, 1111–1122 (2015).
50. Meissner, B. *et al.* The E3 ubiquitin ligase UBR5 is recurrently mutated in mantle cell lymphoma. *Blood* **121**, 3161–3164 (2013).
51. Love, C. *et al.* The genetic landscape of mutations in Burkitt lymphoma. *Nat. Genet.* **44**, 1321–1325 (2012).
52. Weniger, M. A. & Küppers, R. NF-κB deregulation in Hodgkin lymphoma. *Semin. Cancer Biol.* **39**, 32–39 (2016).

66. Gross, A. & Katz, S. G. Non-apoptotic functions of BCL-2 family proteins. *Cell Death Differ.* **24**, 1348–1358 (2017).
67. Meynet, O. *et al.* Caloric restriction modulates Mcl-1 expression and sensitizes lymphomas to BH3 mimetic in mice. *Blood* **122**, 2402–2411 (2013).
68. Chukkapalli, V., Gordon, L. I., Venugopal, P., Borgia, J. A. & Karmali, R. Metabolic changes associated with metformin potentiates Bcl-2 inhibitor, Venetoclax, and CDK9 inhibitor, BAY1143572 and reduces viability of lymphoma cells. *Oncotarget* **9**, 21166–21181 (2018).
69. Kerkela, R. *et al.* Sunitinib-Induced Cardiotoxicity Is Mediated by Off-Target Inhibition of AMP-Activated Protein Kinase. *Clin. Transl. Sci.* **2**, 15–25 (2009).
70. Mihalyova, J. *et al.* Venetoclax: A new wave in hematooncology. *Exp. Hematol.* **61**, 10–25 (2018).

Table 2. Primers for isogenic cell lines

Name	sgRNA Target Sequence	F1	R1
BAK1 gRNA1	AAGACCCTTACCAGAAGCAG	TTGTGGAAAGGACGAAACACCGCCCATCTCTGCTTTTTCTCG	TCTACTATTCTTTCCCCTGCACTGTTGATTGGCCAGCTTACTTCC
BAK1 gRNA2	GGTAGACGTGTAGGGCCAGA	TTGTGGAAAGGACGAAACACCGGGGCTCTCCACCAATGCTA	TCTACTATTCTTTCCCCTGCACTGTGTACCACAAACTGGCCCAAC
BAX gRNA1	TCGGAAAAAGACCTCTCGGG	TTGTGGAAAGGACGAAACACCGCTTGGGGCTCAGTCTCCTTA	TCTACTATTCTTTCCCCTGCACTGTCCTGAGAGCAGGGATGTAGC
BAX gRNA2	AGTAGAAAAGGGCGACAACC	TTGTGGAAAGGACGAAACACCGGCACTGGTTCTCCTCTCTCCT	TCTACTATTCTTTCCCCTGCACTGTCACTTTACTTCACCCCTGCAC
NFKBIA gRNA1	GGTTGGTGATCACAGCCAAG	TTGTGGAAAGGACGAAACACCGCCTGTCTAGGAGGAGCAGCA	TCTACTATTCTTTCCCCTGCACTGTGCATCCAATAGGCACTTTGC
NFKBIA gRNA2	CTGGACGACCGCCACGACAG	TTGTGGAAAGGACGAAACACCGCCAGCCAGCGTTTATAGGG	TCTACTATTCTTTCCCCTGCACTGTCTTATGCAACCGGGGACTT
PMAIP1 gRNA1	TCGAGTGTGCTACTCAACTC	TTGTGGAAAGGACGAAACACCGCAGGTGCACATAAAGCCAAA	TCTACTATTCTTTCCCCTGCACTGTCAAGGGTCTTCCATTCTTGC
PMAIP1 gRNA2	TTCTTGCGCGCCTTCTTCCC	TTGTGGAAAGGACGAAACACCGCAGGACTGTTCGTGTTCAGC	TCTACTATTCTTTCCCCTGCACTGTGCGAGGAGGAAAGAGAGGAG
IKZF5 gRNA1	AGTTACTTCGATCACTGCAG	TTGTGGAAAGGACGAAACACCGTGCTTATGAGCGTCATCTGG	TCTACTATTCTTTCCCCTGCACTGTTCAGGGCAGGGAACTACATC
IKZF5 gRNA2	ATCAGCTCTCGACTCTAGCA	TTGTGGAAAGGACGAAACACCGCCACGAAATCCCAAATATCC	TCTACTATTCTTTCCCCTGCACTGTCTTGGCTGGCTGTTTCCTAT
ID3 gRNA1	CTGGTACCCGGAGTCCCGAG	TTGTGGAAAGGACGAAACACCGAGCGGGACTTCTTTTGGTTT	TCTACTATTCTTTCCCCTGCACTGTGCCGTTTAAACCTCCCTCTC
ID3 gRNA2	TGGCCAGACTGCGTTCCGAC	TTGTGGAAAGGACGAAACACCGAGCGGGACTTCTTTTGGTTT	TCTACTATTCTTTCCCCTGCACTGTCTGGGTGTTCAGCCCTGT
EP300 gRNA1	GTGGCACGAAGATATTACTC	TTGTGGAAAGGACGAAACACCGTTGGTGACCCCTTTTTGAAG	TCTACTATTCTTTCCCCTGCACTGTTGAGCTGAGGCCTAGTTTTTC
EP300 gRNA2	ATGGTGAACCATAAGGATTG	TTGTGGAAAGGACGAAACACCGCTGTCTTTGTGAACTTGGAAGTGA	TCTACTATTCTTTCCCCTGCACTGTCTCCTGTTTGGATCAACATGC
NFIA gRNA1	TCCAGACTTTATCTGCCTGG	TTGTGGAAAGGACGAAACACCGCGACCCGAATATCGAGAGG	TCTACTATTCTTTCCCCTGCACTGTCTCAGGAAGAATCCGGCATA
NFIA gRNA2	CCCTGGATTAGAGCATTGTG	TTGTGGAAAGGACGAAACACCGAGTCTGGAGGTTGGACCTTG	TCTACTATTCTTTCCCCTGCACTGTAGGGTTTTCACGAGGCTTCT
OTUD5 gRNA1	CGGCGCAGGCTACAACAGTG	TTGTGGAAAGGACGAAACACCGGTGTGGGTGGTGCCGTAG	TCTACTATTCTTTCCCCTGCACTGTCAGGGACTGGAATGACGACT
OTUD5 gRNA2	GGTTGTGCGAAAGCATTGCA	TTGTGGAAAGGACGAAACACCGGGCATCTCTGACCCTAGCTG	TCTACTATTCTTTCCCCTGCACTGTTCCCATGGAATGTGTTGATG
BCL2L11 gRNA1	TATGGATCGCCCAAGAGTTG	TTGTGGAAAGGACGAAACACCGTGGACCACAATGTGATTTTTG	TCTACTATTCTTTCCCCTGCACTGTTGCACAAGGGGAGTACAGAA
BCL2L11 gRNA2	GTTCTGATGCAGCTTCCATG	TTGTGGAAAGGACGAAACACCGGAGTGTGTGAGATGGGCTTG	TCTACTATTCTTTCCCCTGCACTGTGTCTGTGCTCATAAAATTCCTTTGC
UBR5 gRNA1	TTGTTGTCTAAGAACGACGA	TTGTGGAAAGGACGAAACACCGCCAATTCATAAAGCAGTAGCTTAGG	TCTACTATTCTTTCCCCTGCACTGTCATCACAAATGCTCAAAGAGAG
UBR5 gRNA2	GCAACCAAGATAATGCTAGT	TTGTGGAAAGGACGAAACACCGTCCTACCCCCTATGCCTTCT	TCTACTATTCTTTCCCCTGCACTGTCTCTGACTGCACCACTGGAA
TP53 gRNA1	GGATGATTTGATGCTGTCCC	TTGTGGAAAGGACGAAACACCGCTGGTAAGGACAAGGGTTGG	TCTACTATTCTTTCCCCTGCACTGTGCCAAAGGGTGAAGAGGAAT
TP53 gRNA4	AGACGGAAACCGTAGCTGCC	TTGTGGAAAGGACGAAACACCGGAAGACCCAGGTCCAGATGA	TCTACTATTCTTTCCCCTGCACTGTTCAAAAGCCAAGGAATACACG

Table 4. Sample characteristics. Mononuclear cells were isolated with Ficoll/Hypaque density-gradient centrifugation, cryopreserved with 10% DMSO and stored in vapor-phase liquid nitrogen until the time of analysis. MCs, mononuclear cells; PB, peripheral blood; FFPE, formalin-fixed, paraffin-embedded.

Patient	Pre-venetoclax sample	Post-venetoclax sample	Germline sample
1	Marrow MCs	Marrow MCs	saliva
2	PBMCs	PBMCs	saliva
3	FFPE marrow biopsy	FFPE marrow biopsy	absent
4	FFPE marrow biopsy	Fresh lymph node biopsy	saliva
5	PBMCs	PBMCs	saliva
6	PBMCs	PBMCs	saliva

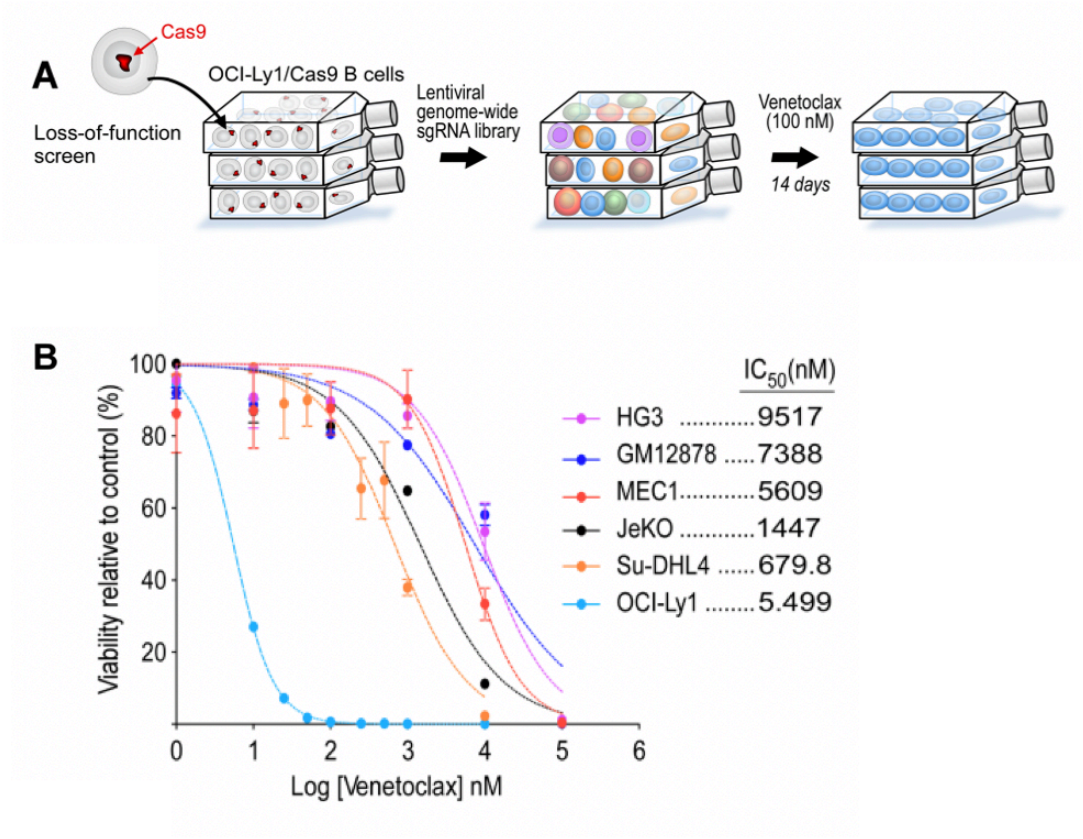

Figure 2. Setup of CRISPR-Cas9 loss-of-function genome-wide screen for genes driving venetoclax resistance

(A) Experimental schema of the knockout screen using the BCL-2 driven OCI-Ly1 cell line (two biologically independent replicate experiments).

(B) Dose-response curves of multiple lymphoid cell lines to determine cell line to use for experiments

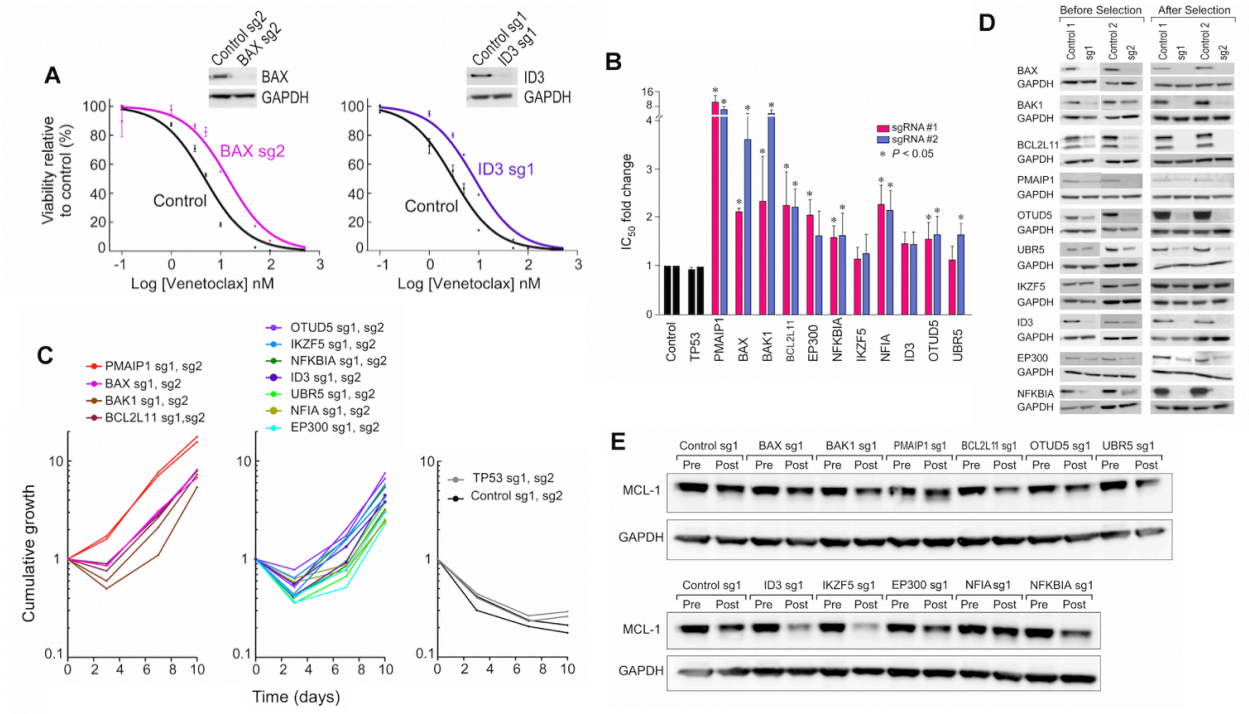

Figure 4. Validation of loss-of-function screen hits through generation of isogenic knockout lines.

(A) Dose-response curves to venetoclax of 2 representative knockout OCI-Ly1 cells with related western-blots for quantification of the target protein.

(B) Venetoclax IC50 fold change of single gene knockout isogenic cell lines compared to OCI-Ly1 cells transduced with control sgRNAs. Data are mean +/- s.e.m., **P* from extra sum-of-squares F test.

(C) Cumulative growth over time of each of the genetically perturbed OCI-Ly1 cells under venetoclax (100 nM) treatment.

(D) Protein expression levels in single gene knockout isogenic cell lines (2 lines per gene), before and after selection with venetoclax.

(E) Western-blot for quantification of MCL-1 in genetically perturbed OCI-Ly1 cell lines before and after 2 weeks of venetoclax exposure.

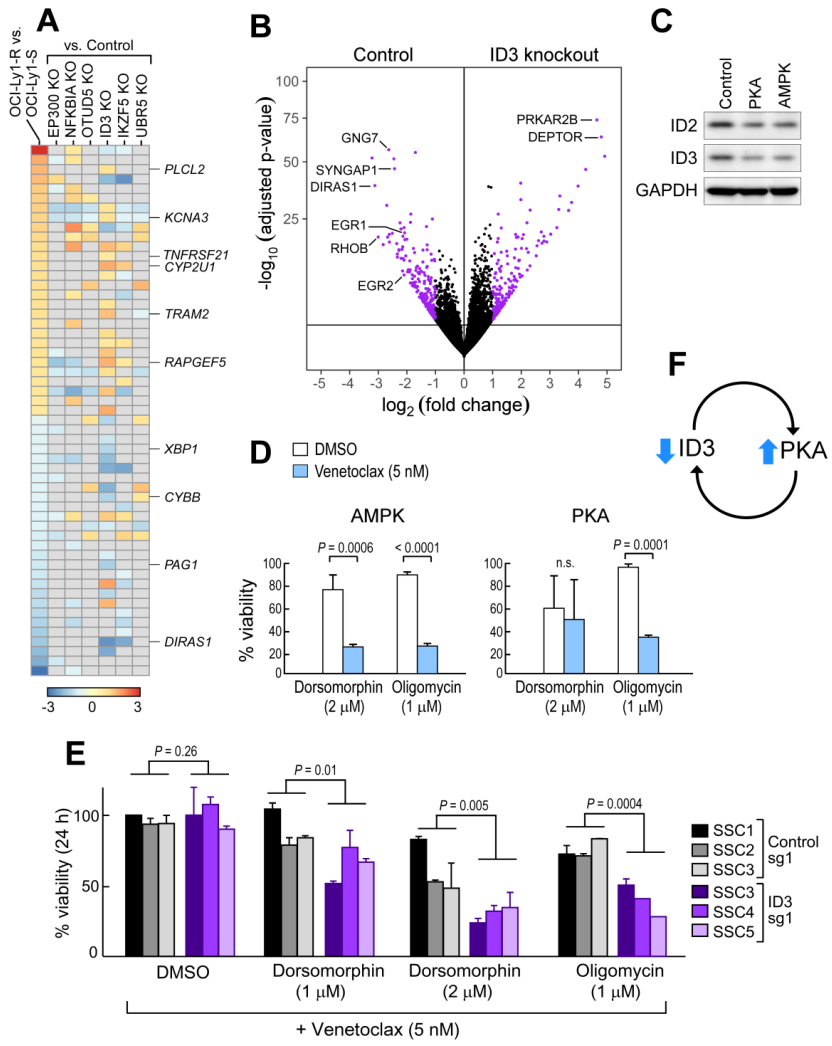

Figure 6. A circuit of ID3 repression and PKA-AMPK deregulation is implicated in venetoclax resistance.

(A) Heatmap of differentially expressed transcripts between the OCI-Ly1-S and OCI-Ly1-R cells, and of knockout (KO) cell lines from the screen hits vs cell lines with KO using non-targeting sgRNAs. Genes affected in common with the OCI-Ly1-S and –R cells and in the ID3 KO line are indicated.

(B) Volcano plot of transcripts changes in ID3 KO OCI-Ly1 cells compared to non-targeting sgRNA transduced OCI-Ly1 cells.

(C) Western-blot for quantification of ID2 and ID3 proteins in *PRKAR2B* (PKA) and *PRKAA2* (AMPK) overexpressing OCI-Ly1 cell lines.

(D) Sensitivity of AMPK and PKA overexpressing cells to venetoclax when used in combination with dorsomorphin (2 μM) and oligomycin (1 μM), compared to DMSO control. Data are mean +/- s.e.m. from three biologically independent experiments, p-value is from two-sided t-test.

(E) Viability at 24 hours of single-cell clones from ID3 knockout OCI-Ly1 cells compared to non-targeting sgRNAs transduced OCI-Ly1 cells after exposure to dorsomorphin and oligomycin in addition to venetoclax. Data are mean +/- s.d. from three biologically independent experiments and p-values are from ANOVA test.

(F) Schema of the ID3 and PKA resistance circuit

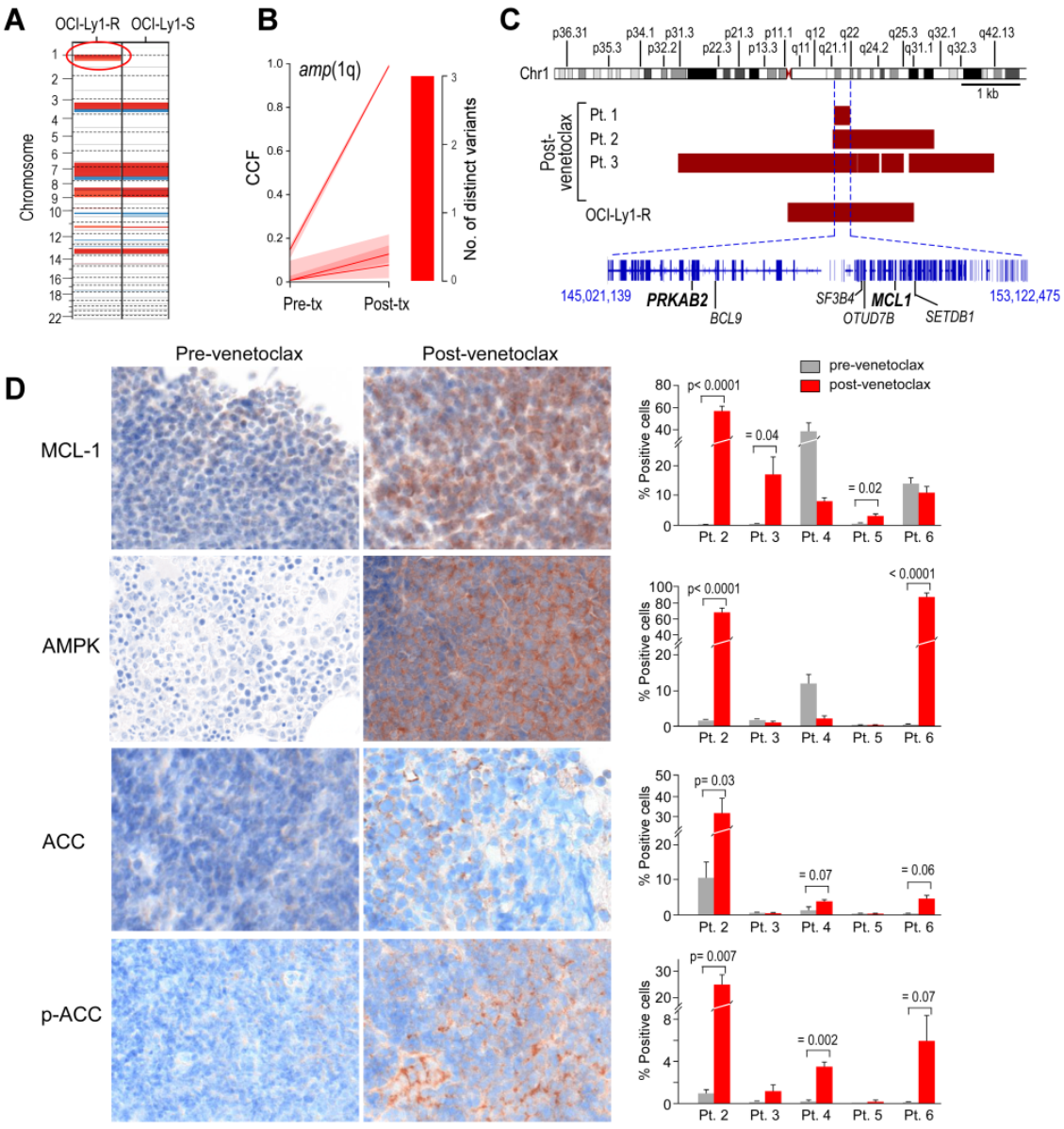

Figure 8. Alterations in MCL-1 expression and AMPK signaling detected in both the OCI-Ly1 resistant cell line and CLL samples from patients with venetoclax resistance
(A) Comparison of somatic copy number variations in the OCI-Ly1-S and OCI-Ly1-R cells (gain in red, loss in blue).
(B) Comparison (modal CCF with 95% CI) between pre-treatment and relapse samples for *amp*(1q).
(C) Representation of the minimal gained region in the 1q locus across both the OCI-Ly1 cell lines and relapsed samples from Patients 1, 2 and 3.
(D) Immunohistochemical stains of patient samples before and after progression on venetoclax for MCL-1, AMPK, ACC, and p-ACC, with representative images from Patient 2 (left), and quantitation of % positively staining cells before (grey) and after (red) venetoclax treatment for Patients 2-6 (right). Data are mean +/- s.e.m. from replicates; p-value is from Welch t-test.